Novel mechanisms of the transformations of the G·C base pairs in Watson-Crick and Hoogsteen configurations via the mutual rotations of the bases and proton transfer: A quantum-chemical investigation

Ol'ha Brovarets' (o.o.brovarets@gmail.com)

Institute of Molecular Biology and Genetics National Academy of Sciences of Ukraine: Institut molekularnoi biologii i genetiki Nacional'na akademia nauk Ukraini https://orcid.org/0000-0002-8929-293X

Alona Muradova

Taras Shevchenko National University of Kyiv: Kiivs'kij nacional'nij universitet imeni Tarasa Sevcenka

Dmytro Hovorun

Institute of Molecular Biology and Genetics National Academy of Sciences of Ukraine: Institut molekularnoi biologii i genetiki Nacional'na akademia nauk Ukraini

Research Article

Keywords: G·C base pair, DNA, RNA, Structural biology, Conformer, Tautomer, Proton transfer, Quantum-chemical calculations

Posted Date: May 18th, 2022

DOI: https://doi.org/10.21203/rs.3.rs-1322909/v1

Abstract

In this study for the first time at the MP2/6-311++G(2df,pd)//B3LYP/6-311++G(d,p) level of theory it was comprehensively investigated unusual conformationally-tautomeric transformations of the G*·C*(WC), G*·C*(rWC), G*·C*^{t}(rWC), G*^{t}·C*(rH) and G*^{t}·C*^{t}(rH) base pairs - G*·C*(WC)↔G*^{t}·C(rw_H)$_{\uparrow}$↔G*$_{N7}$·C*(rw_H)$_{\uparrow}$↔G*$_{N7}$·C*(w_H)$_{\uparrow}$↔G*^{t}·C*$_{O2}$(w_H)$_{\uparrow}$↔

G*^{t}·C*$_{O2}$(rw_H)$_{\uparrow}$, G*·C*(rWC)↔G*^{t}·C*$_{O2}$(rw_{WC})$_{\downarrow}$/↔G*^{t}·C*$_{O2}$(w_H)$_{\uparrow}$, G*·C*^{t}(rWC)↔G*^{t}·C*$^{t}_{O2}$(w_H)$_{\downarrow}$↔G*^{t}·C*$^{t}_{O2}$(rw_H)$_{\downarrow}$/↔G*^{t}·C*$^{t}_{O2}$(rw_{WC})$_{\downarrow}$↔G*^{t}·C*$^{t}_{O2}$(w_{WC})$_{\downarrow}$, G*^{t}·C*(rH)↔G*·C*$_{O2}$(w_{WC})$_{\uparrow}$/↔G*·C*$_{O2}$(w_H)$_{\downarrow}$ and G*^{t}·C*^{t}(rH)↔G*·C*$^{t}_{O2}$(w_{WC})$_{\uparrow}$/

↔G*·C*$^{t}_{O2}$(rw_H)$_{\downarrow}$↔G*·C*$^{t}_{O2}$(w_H)$_{\downarrow}$. It was reliably established that they occur through the mutual rotations of the G and C bases around intermolecular H-bonds and proton transfer along the intermolecular H-bonds. These novel conformationally-tautomeric tranformations are intrinsically inherent properties of the Watson-Crick (WC) and Hoogsteen (H) G·C base pairs and lead to their transformation into the wobble (w) or reverse wobble (rw) base pairs. These conformationally-tautomeric transformations of the G·C base pairs are accompanied by the rearrangement of the intermolecular H-bonds and changing of the dipole moments.

Introduction

Investigation of the G·C base pair attracts active interest over the years [1-5], since, from the one side, it is a building block of the DNA molecule [6], while from the other side – its unusual conformers can become a part of the structure of the RNA molecule [7-12].

These unusual conformers of the G·C base pair can be formed due to the involvement of the rare tautomeric forms (tautomers) [13-21] of the G and C bases in different combinations. However, the source of the origin of the rare tautomers of the G and C bases are still precisely unknown.

In the literature data, it was found out that G* and C* rare tautomers can arise directly within the base pair due to the several mechanisms:

1. G·C↔G*·C* Lowdin's mechanism [22-26], occurring through the proton transfer along the intermolecular N4H…O6 and N1H…N3 H-bonds;
2. 4 H_2O·G·C↔4 H_2O·G*·C*^{t}, 6 H_2O·G·C↔6 H_2O·G*·C*^{t} and 11 H_2O·G·C↔11 H_2O·G*·C*^{t} mechanism [27], occurring through the proton transfer, mediated by several water molecules;
3. G·C(WC)↔G·C*$_{\uparrow}$(w)/G*·C$_{\downarrow}$(w)/G·C*$_{\downarrow}$(w)/G*·C$_{\uparrow}$(w) [28] and G*·C*(rWC)↔G·C*$_{O2}$(rWC)↔G·C*(rw_{WC})↔G*·C(rw_{WC})/G*$_{N2}$·C(rWC)/G*$^{t}_{N2}$·C(rWC)/ G*$_{N2}$·C*(rw_{WC})↔G*·C*$_{O2}$(rw_{WC}), G*^{t}·C*(H)↔G*$_{N7}$·C(H)↔G*^{t}·C*$_{O2}$(w_H)↔G*$_{N7}$·C*(w_H)/ G*^{t}·C(w_H)↔G*$^{t}_{N7}$·C*(w_H), G*^{t}·C*(rH)↔G*$^{t}_{N7}$·C(rH)/G*^{t}·C*$_{O2}$(rw_H)↔G*$^{t}_{N7}$·C*(rw_H)/ G*^{t}·C*(rw_H)↔G*$_{N7}$·C*(rw_H) [29, 30] mechanisms ,

occurring through the intermolecular proton transfer and relative shifting of the bases, which finally lead to the novel biologically important G·C nucleobase pairs in Watson-Crick, Hoogsteen and wobble configurations, that conformationally interconvert through the mutual rotations of the bases around the intermolecular H-bonds [31].

As a result of these comprehensive investigations, it was revealed various novel conformers of the G·C base pair by the participation of the rare tautomers. However, reaction pathways, interconnecting them, have not been widely presented so far.

In this work we aimed to established conformationally-tautomeric pathways of the interconversion of the different unusual G·C base pairs.

As a result of this investigation, it was found out novel reaction pathways of the conformationally-tautomeric transformations of the Lowdin G*·C*(WC), reverse Lowdin G*·C*(rWC), G*·C*^{t}(rWC), reverse Hoogsteen G*^{t}·C*(rH), G*^{t}·C*^{t}(rH) base pairs into the wobble (w) and reverse wobble (rw) base pairs bounded from the Watson-Crick and Hoogsteen edges, which are accompanied by the change of the dipole moment of the considered base pairs and TSs (2.25-11.12 D) and rearrangement of the intermolecular H-bonds.

Computational Methods

Density functional theory calculations of the geometry and vibrational frequencies. Equilibrium geometries of the investigated G·C base pairs and transition states (TSs) of their mutual conformational or tautomeric transformations, as well as their harmonic vibrational frequencies have been calculated, using Gaussian'09 program package [32] at the B3LYP/6-311++G(d,p) level of theory [33-37], which approved itself successfully for the calculations of the similar systems and processes and shown acceptable level of accuracy and adequacy of the obtained results [37, 38]. A scaling factor that is equal to 0.9668 has been applied in the present work for the correction of the harmonic frequencies for all complexes [30, 31, 39].

We have confirmed local minima and TSs, localized by Synchronous Transit-guided Quasi-Newton method [40], on the potential energy landscape by the absence or presence, respectively, of one imaginary frequency in the vibrational spectra of the complexes. All reaction pathways have been reliably confirmed by providing intrinsic reaction coordinate (IRC) calculations [40] from each TS in the forward and reverse directions at the B3LYP/6-311++G(d,p) level of theory.

All calculations have been performed in the continuum with ε=1, that adequately reflects the processes occurring in real biological systems without deprivation of the structurally-functional properties of the bases in the composition of the DNA or RNA molecules and satisfactorily models the substantially hydrophobic recognition pocket of the DNA-polymerase machinery as a part of the replisome [41, 42].

Single point energy calculations. We continued geometry optimizations with electronic energy calculations as the single point calculations at the MP2/6-311++G(2df,pd) level of theory [43, 44].

The Gibbs free energy G for all structures was obtained in the following way:

$$G=E_{el}+E_{corr}, \quad (1)$$

where E_{el} – electronic energy and E_{corr} – thermal correction.

QTAIM analysis. Bader's quantum theory of Atoms in Molecules (QTAIM) [45] was applied to analyse the electron density distribution, using program package AIMAll [46]. The presence of the bond critical point (BCP), namely the so-called (3,-1) BCP, and a bond path between the donor and acceptor of the H-bond, as well as the positive value of the Laplacian at this BCP ($\Delta\rho>0$), were considered as criteria for the formation of the H-bond [47-50]. Wave functions were obtained at the B3LYP/6-311++G(d,p) level of theory, used for geometry optimisation.

The atomic numbering scheme for the DNA bases is conventional and rare tautomeric forms of the G and C bases are marked by an asterisk (*) [14].

Obtained results and their discussion.

Obtained results are presented on Fig. 1 and in Table 1, which detailed discussion are outlined below.

Altogether, it was established five novel routes of the conformationally-tautomeric transformations of the G·C base pairs – 1. $G^{*}\cdot C^{*}(WC)\leftrightarrow G^{*t}\cdot C(rw_H)_{\uparrow}\leftrightarrow G^{*}_{N7}\cdot C^{*}(rw_H)_{\uparrow}\leftrightarrow G^{*}_{N7}\cdot C^{*}(w_H)_{\uparrow}\leftrightarrow G^{*t}\cdot C^{*}_{O2}(w_H)_{\uparrow}\leftrightarrow G^{*t}\cdot C^{*}_{O2}(rw_H)_{\uparrow}$, 2. $G^{*}\cdot C^{*}(rWC)\leftrightarrow G^{*t}\cdot C^{*}_{O2}(rw_{WC})_{\downarrow}/\leftrightarrow G^{*t}\cdot C^{*}_{O2}(w_H)_{\uparrow}$, 3. $G^{*}\cdot C^{*t}(rWC)\leftrightarrow G^{*t}\cdot C^{*t}_{O2}(w_H)_{\downarrow}\leftrightarrow G^{*t}\cdot C^{*t}_{O2}(rw_H)_{\downarrow}/\leftrightarrow G^{*t}\cdot C^{*t}_{O2}(rw_{WC})_{\downarrow}\leftrightarrow G^{*t}\cdot C^{*t}_{O2}(w_{WC})_{\downarrow}$, 4. $G^{*t}\cdot C^{*}(rH)\leftrightarrow G^{*}\cdot C^{*}_{O2}(w_{WC})_{\uparrow}/\leftrightarrow G^{*}\cdot C^{*}_{O2}(w_H)_{\downarrow}$ and 5. $G^{*t}\cdot C^{*t}(rH)\leftrightarrow G^{*}\cdot C^{*t}_{O2}(w_{WC})_{\uparrow}/\leftrightarrow G^{*}\cdot C^{*t}_{O2}(rw_H)_{\downarrow}\leftrightarrow G^{*}\cdot C^{*t}_{O2}(w_H)_{\downarrow}$ (Fig. 1 and Table 1).

General feature of these reactions of the transformations of the WC/H base pairs is that they start from the rotations of the G·C base pairs around the intermolecular H-bonds, which is further followed by the proton transfer (PT) along the intermolecular neighboring H-bonds (Fig. 1 and Table 1).

So, let's analyze step-by-step revealed pathways in more details.

1. The $G^{*}\cdot C^{*}(WC)\leftrightarrow G^{*}\cdot C^{*}(rw_{WC/H})\leftrightarrow G^{*t}\cdot C(rw_{WC/H})\leftrightarrow G^{*t}\cdot C(rw_H)_{\uparrow}\leftrightarrow G^{*}_{N7}\cdot C^{*}(rw_H)_{\uparrow}\leftrightarrow G^{*}_{N7}\cdot C^{*}(w_H)_{\uparrow}\leftrightarrow G^{*t}\cdot C^{*}_{O2}(w_H)_{\uparrow}\leftrightarrow G^{*t}\cdot C^{*}_{O2}(rw_H)_{\uparrow}$ reaction pathway leads to the formation of the wobble (w_H) or reverse wobble (rw_H) base pairs, which bind from the Hoogsteen side, and consists from seven stages (Fig. 1a). This conformationally-tautomeric transformation starts from the

rotation of the bases within the Lowdin G*·C*(WC) base pair around the upper (G)O6H…N4(C) H-bond, leading to the formation of the G*·C*($rw_{WC/H}$) base pair - G*·C*(WC)↔G*·C*($rw_{WC/H}$).

Further, formed G*·C*($rw_{WC/H}$) base pair transforms through the proton transfer along the intermolecular O6H…N4 and N3H…O6 H-bonds into the G*·C*($rw_{WC/H}$) base pair - G*·C*($rw_{WC/H}$)↔G^{*t}·C($rw_{WC/H}$), which is accompanied by the changing of the orientation of the O6H hydroxyl group of the G base from *cis*- to *trans*-.

Formed G^{*t}·C($rw_{WC/H}$) base pair transforms through the mutual rotation of the bases around the middle intermolecular (G)O6H…N3(C) H-bond - G^{*t}·C($rw_{WC/H}$)↔G^{*t}·C$(rw_H)_{\uparrow}$. Novel reverse wobble Hoogsteen G^{*t}·C$(rw_H)_{\uparrow}$ base pair launches cascade of the interconversions between the wobble Hoogsteen (G^*_{N7}·C*$(w_H)_{\uparrow}$, G^{*t}·$C^*_{O2}(w_H)_{\uparrow}$) and reverse wobble Hoogsteen base pairs (G^{*t}·C$(rw_H)_{\uparrow}$, G^*_{N7}·C*$(rw_H)_{\uparrow}$, G^{*t}·$C^*_{O2}(rw_H)_{\uparrow}$), occurring through the proton transfer and rotations of the bases - G^{*t}·C$(rw_H)_{\uparrow}$↔G^*_{N7}·C*$(rw_H)_{\uparrow}$↔G^*_{N7}·C*$(w_H)_{\uparrow}$↔G^{*t}·$C^*_{O2}(w_H)_{\uparrow}$↔G^{*t}·$C^*_{O2}(rw_H)_{\uparrow}$ (Fig. 1a).

Notably, that during this G*·C*(WC)↔G^{*t}·$C^*_{O2}(rw_H)_{\uparrow}$ transformation dipole moment μ of the complex varies in the wide range of values – 2.36-11.12 D, reaching its maximum at the TSs – $TS_{G^*\cdot C^*(rwWC/H)\leftrightarrow G^{*t}\cdot C(rwWC/H)}$ (μ=10.48 D), $TS_{G^{*t}\cdot C(rwWC/H)\leftrightarrow G^{*t}\cdot C(rwH)\uparrow}$ (μ=8.84 D), $TS_{G^{*t}\cdot C(rwH)\uparrow\leftrightarrow G^*N7\cdot C^*(rwH)\uparrow}$ (μ=11.12 D) and $TS_{G^*N7\cdot C^*(rwH)\uparrow\leftrightarrow G^*N7\cdot C^*(H)\uparrow}$ (μ=9.46 D), indicating their high polarization.

1. The G*·C*(rWC)↔G*·C*($w_{WC/H}$)↔G^{*t}·$C^*_{O2}(w_{WC/H})$↔G^{*t}·$C^*_{O2}(rw_{WC})_{\downarrow}$/↔$G^{*t}$·$C^*_{O2}(w_H)_{\uparrow}$ reaction pathway starts from the rotation of the bases within the reverse Lowdin G*·C*(rWC) base pair and further splits into two pathways – G^{*t}·$C^*_{O2}(w_{WC/H})$↔G^{*t}·$C^*_{O2}(rw_{WC})_{\downarrow}$ and G^{*t}·$C^*_{O2}(w_{WC/H})$↔G^{*t}·$C^*_{O2}(w_H)_{\uparrow}$, leading to the formations of the reverse wobble Watson-Crick G^{*t}·$C^*_{O2}(rw_{WC})_{\downarrow}$ and wobble Hoogsteen G^{*t}·$C^*_{O2}(w_H)_{\uparrow}$ base pairs, accordingly (Fig. 1b).

This division occurs at the so-called bifurcation point – G^{*t}·$C^*_{O2}(w_{WC/H})$, which arises after the proton transfer – G*·C*($w_{WC/H}$)↔G^{*t}·$C^*_{O2}(w_{WC/H})$, accompanied by *cis*→*trans*-transition of the O6H hydroxyl group of the G* base. Following the 1st route – G^{*t}·$C^*_{O2}(w_{WC/H})$↔G^{*t}·$C^*_{O2}(rw_{WC})_{\downarrow}$ – this bifurcation point transforms into the reverse wobble Watson-Crick G^{*t}·$C^*_{O2}(rw_{WC})_{\downarrow}$ base pair, while following the 2nd route – it comes to the wobble Hoogsteen G^{*t}·$C^*_{O2}(w_H)_{\uparrow}$ base pair. Notably, that both formed G^{*t}·$C^*_{O2}(rw_{WC})_{\downarrow}$ and G^{*t}·$C^*_{O2}(w_H)_{\uparrow}$ base pairs are almost iso-energetical, since their relative Gibbs free energies consist ΔG=16.83 and 16.02 kcal·mol^{-1}, accordingly.

The minimum values of the dipole moment μ of these complexes is achieved for the G^{*t}·$C^*_{O2}(rw_{WC})_{\downarrow}$ base pair (μ=2.25 D), while the maximum value – for the $TS_{G^{*t}\cdot C^*O2(wWC/H)\leftrightarrow G^{*t}\cdot C^*O2(wH)\uparrow}$ (μ=7.55 D).

1. The $G^{*}\cdot C^{*t}(rWC)\leftrightarrow G^{*}\cdot C^{*t}(w_{WC/H})\leftrightarrow G^{*t}\cdot C^{*t}{}_{O2}(w_{WC/H})\leftrightarrow G^{*t}\cdot C^{*t}{}_{O2}(w_{H})_{\downarrow}\leftrightarrow G^{*t}\cdot C^{*t}{}_{O2}(rw_{H})_{\downarrow}/\leftrightarrow G^{*t}\cdot C^{*t}{}_{O2}(rw_{WC})_{\downarrow}\leftrightarrow G^{*t}\cdot C^{*t}{}_{O2}(w_{WC})_{\downarrow}$ reaction pathway leads to the $G^{*t}\cdot C^{*t}{}_{O2}(rw_{H})_{\downarrow}$ and $G^{*t}\cdot C^{*t}{}_{O2}(w_{WC})_{\downarrow}$ base pairs, accordingly (Fig. 1c). It proceeds through the bifurcation point – $G^{*t}\cdot C^{*t}{}_{O2}(w_{WC/H})$ base pair, which arises after the $G^{*}\cdot C^{*t}(w_{WC/H})\leftrightarrow G^{*t}\cdot C^{*t}{}_{O2}(w_{WC/H})$ transformation through the proton transfer in the $G^{*}\cdot C^{*t}(w_{WC/H})$ base pair.

This $G^{*t}\cdot C^{*t}{}_{O2}(w_{WC/H})$ base pair launches two separate routes of the cascade transformations through the rotations of the bases around the intermolecular H-bonds, leading to the shifting of the base on the right down:

- $G^{*t}\cdot C^{*t}{}_{O2}(w_{WC/H})\leftrightarrow G^{*t}\cdot C^{*t}{}_{O2}(w_{H})_{\downarrow}\leftrightarrow G^{*t}\cdot C^{*t}{}_{O2}(rw_{H})_{\downarrow}$;
- $G^{*t}\cdot C^{*t}{}_{O2}(w_{WC/H})\leftrightarrow G^{*t}\cdot C^{*t}{}_{O2}(rw_{WC})_{\downarrow}\leftrightarrow G^{*t}\cdot C^{*t}{}_{O2}(w_{WC})_{\downarrow}$.

Maximum values of the dipole moment μ are achieved at the $G^{*t}\cdot C^{*t}{}_{O2}(w_{H})_{\downarrow}$ (μ=7.64 D), $G^{*t}\cdot C^{*t}{}_{O2}(rw_{WC})_{\downarrow}$ (μ=4.88 D), $G^{*t}\cdot C^{*t}{}_{O2}(w_{WC})_{\downarrow}$ (μ=5.26) base pairs and $TS_{G^{*t}\cdot C^{*t}O2(wH)\downarrow\leftrightarrow G^{*t}\cdot C^{*t}O2(rwH)\downarrow}$ (μ=8.04 D) (Fig. 1c).

1. Joint feature of the $G^{*t}\cdot C^{*}(rH)\leftrightarrow G^{*t}\cdot C^{*}(w_{WC/H})\leftrightarrow G^{*}\cdot C^{*}{}_{O2}(w_{WC/H})\leftrightarrow G^{*}\cdot C^{*}{}_{O2}(w_{WC})_{\uparrow}/\leftrightarrow G^{*}\cdot C^{*}{}_{O2}(w_{H})_{\downarrow}$ (Fig. 1d) and $G^{*t}\cdot C^{*t}(rH)\leftrightarrow G^{*t}\cdot C^{*t}(w_{WC/H})\leftrightarrow G^{*}\cdot C^{*t}{}_{O2}(w_{WC/H})\leftrightarrow G^{*}\cdot C^{*t}{}_{O2}(w_{WC})_{\uparrow}/\leftrightarrow G^{*}\cdot C^{*t}{}_{O2}(rw_{H})_{\downarrow}\leftrightarrow G^{*}\cdot C^{*t}{}_{O2}(w_{H})_{\downarrow}$ (Fig. 1e) transformations of the reverse Hoogsteen $G^{*t}\cdot C^{*}(rH)$ and $G^{*t}\cdot C^{*t}(rH)$ base pairs, respectively, is that they both start from the mutual rotations of the bases around the upper (G)O6H…O2(C) H-bond and further continue with the proton transfer along the intermolecular N3H…O6 and O6H…O2 H-bonds, leading to the so-called bifurcation point – $G^{*}\cdot C^{*}{}_{O2}(w_{WC/H})$ and $G^{*}\cdot C^{*t}{}_{O2}(w_{WC/H})$ base pairs, respectively.

After that, reaching the so-called bifurcation point, each of these reactions divides into two routes. The 1st route – $G^{*}\cdot C^{*}{}_{O2}(w_{WC/H})\leftrightarrow G^{*}\cdot C^{*}{}_{O2}(w_{WC})_{\uparrow}$ and $G^{*}\cdot C^{*t}{}_{O2}(w_{WC/H})\leftrightarrow G^{*}\cdot C^{*t}{}_{O2}(w_{WC})_{\uparrow}$, respectively, occurs through the mutual rotations of the bases around the (G)O6H…N3(C) H-bond and leads to the formation of the $G^{*}\cdot C^{*}{}_{O2}(w_{WC})_{\uparrow}$ and $G^{*}\cdot C^{*t}{}_{O2}(w_{WC})_{\uparrow}$ base pairs, respectively (Figs. 1d and 1e). The 2nd route interconnects the formed $G^{*}\cdot C^{*}{}_{O2}(w_{WC/H})$ and $G^{*}\cdot C^{*t}{}_{O2}(w_{WC/H})$ base pairs with various base pairs through the cascade of the rotational transformations – $G^{*}\cdot C^{*}{}_{O2}(w_{WC/H})\leftrightarrow G^{*}\cdot C^{*}{}_{O2}(w_{H})_{\downarrow}$ and $G^{*}\cdot C^{*t}{}_{O2}(w_{WC/H})\leftrightarrow G^{*}\cdot C^{*t}{}_{O2}(rw_{H})_{\downarrow}\leftrightarrow G^{*}\cdot C^{*t}{}_{O2}(w_{H})_{\downarrow}$, respectively (Figs. 1d and 1e).

Dipole moments reach their maximum values (6.00-7.27 D) at the TSs (Figs. 1d and 1e).

Altogether, these conformationally-tautomeric transformations are accompanied by the re-arrangement of the intermolecular AH…B H-bonds at the base pairs and TSs of their interconversions, reaching their maximal H…B distances (2.505-2.598 Å) at the unusual $G^{*}\cdot C^{*t}{}_{O2}(rw_{H})_{\downarrow}$ and $G^{*}\cdot C^{*t}{}_{O2}(w_{H})_{\downarrow}$ base pairs (Fig. 1e).

Conclusions

In this study for the first time it has been established in detail reaction pathways for the Lowdin G*·C* (WC), reverse Lowdin G*·C*(rWC), G*·C*^{t}(rWC) and reverse Hoogsteen G*^{t}·C*(rH), G*^{t}·C*^{t}(rH) base pairs, occuring through the conformational and tautomeric transformations.

These transformations represent cascade of the interconversions of the various G·C base pairs in Watson-Crick, reverse Watson-Crick, Hoogsteen, reverse Hoogsteen, wobble and reverse wobble configurations through the mutual rotations of the bases and intermolecular proton transfer. Further experimental verification and consideration of the obtained results are suggested.

Declarations

Funding: Not applicable.

Conflicts of interest/Competing interests: Not applicable.

Availability of data and material: Not applicable.

Code availability: Gaussian'09 program package – gaussian.com; AIMAll program package – http://aim.tkgristmill.com/.

Authors' contributions: OB – idea formulation, setting of the task, calculation of the data, building of the graphs, data extrapolation, preparing, and proofreading of the draft of the manuscript. AM – idea formulation, calculation of the data, preparing, and proofreading of the draft of the manuscript. DH – idea formulation, preparing, and proofreading of the draft of the manuscript. All authors contributed to the article and approved the submitted version.

References

1. Brovarets' OO, Hovorun DM (2018) Renaissance of the tautomeric hypothesis of the spontaneous point mutations in DNA: New ideas and computational approaches. Mitochondrial DNA – New Insights / Ed. by Herve Seligmann, London, United Kingdom: IntechOpen, ISBN 978-953-51-6167-7
2. Brovarets' OO, Hovorun DM (2014) Why the tautomerization of the G·C Watson–Crick base pair *via* the DPT does not cause point mutations during DNA replication? QM and QTAIM comprehensive analysis. J Biomol Struct Dynam 32:1474–1499
3. Florian J, Leszczynski J, Spontaneous (1996) DNA mutations induced by proton transfer in the guanine·cytosine base pairs: An energetic perspective. J Am Chem Soc 118:3010–3017
4. Bezbaruah B, Medhi BC (2016) Quantum mechanical study on the proton transfer mechanism within adenine-thymine and guanine-cytosine base pairs of DNA nucleobase. Ind J Adv Chem Sci 4:314–320

5. Gop S, Sutradhar R, Chakraborty S, Sinha TP (2020) Tautomeric effect of guanine on stability, spectroscopic and absorbance properties in cytosine–guanine base pairs: A DFT and TD-DFT perspective. Theor Chem Acc 139:34
6. Crick FHC, Watson JD (1954) The complementary structure of deoxyribonucleic acid. Proc. Roy. Soc., A223, 80-96
7. Heus HA, Hilbers CW (2003) Structures of non-canonical tandem base pairs in RNA helices: Review. Nucleos Nucleot Nucl Acids 22:559–571
8. Mukherjee S, Bansal M, Bhattacharyya D (2006) Conformational specificity of non-canonical base pairs and higher order structures in nucleic acids: Crystal structure database analysis. J Comput Aided Mol Des 20:629–645
9. Das J, Mukherjee S, Mitra A, Bhattacharyya D (2006) Non-canonical base pairs and higher order structures in nucleic acids: Crystal structure database analysis. J Biomol Struct Dynam 24:149–161
10. Sharma P, Mitra A, Sharma S, Singh H, Bhattacharyya D (2008) Quantum chemical studies of structures and binding in noncanonical RNA base pairs: The trans Watson-Crick:Watson-Crick family. J Biomol Struct Dynam 25:709–732
11. Halder S, Bhattacharyya D (2013) RNA structure and dynamics: A base pairing perspective. Prog Biophys Mol Biol 113:264–283
12. Bhattacharya S, Jhunjhunwala A, Halder A, Bhattacharyya D, Mitra A (2019) Going beyond base-pairs: Topology-based characterization of base-multiplets in RNA. RNA 25:573–589
13. Cruz-Cabeza AJ, Groom CR (2011) Identification, classification and relative stability of tautomers in the Cambridge structural database. CrystEngComm 13:93–98
14. Brovarets' OO, Hovorun DM (2010) How stable are mutagenic tautomers of the DNA bases? Biopol. Cell 26:72–76
15. Brovarets' OO, Hovorun DM (2011) Intramolecular tautomerization and the conformational variability of some classical mutagens – cytosine derivatives: Quantum chemical study. Biopol Cell 27:221–230
16. Brovarets' OO, Hovorun DM (2014) DPT tautomerisation of the G·A_{syn} and A*·G*$_{syn}$ DNA mismatches: A QM/QTAIM combined atomistic investigation. Phys Chem Chem Phys 16:9074–9085
17. Brovarets' OO, Hovorun DM (2021) Does the G·G*$_{syn}$ DNA mismatch containing canonical and rare tautomers of the guanine tautomerise through the DPT? A QM/QTAIM microstructural study. Mol Phys 112:3033–3046
18. Brovarets' OO, Zhurakivsky RO, Hovorun DM (2014) Is the DPT tautomerisation of the long A·G Watson-Crick DNA base mispair a source of the adenine and guanine mutagenic tautomers? A QM and QTAIM response to the biologically important question. J Comput Chem 35:451–466
19. Brovarets' OO, Kolomiets' IM, Hovorun DM (2012) Elementary molecular mechanisms of the spontaneous point mutations in DNA: A novel quantum-chemical insight into the classical

understanding. Quantum chemistry – molecules for innovations (Ed. by T. Tada). Rijeka: In Tech Open Access,

20. Brovarets' OO, Hovorun DM (2015) The nature of the transition mismatches with Watson-Crick architecture: The G*·T or G·T* DNA base mispair or both? A QM/QTAIM perspective for the biological problem. J Biomol Struct Dynam 33:925–945
21. Brovarets' OO, Hovorun DM (2015) Tautomeric transition between wobble A·C DNA base mispair and Watson-Crick-like A·C* mismatch: Microstructural mechanism and biological significance. Phys Chem Chem Phys 17:15103–15110
22. Löwdin P-O (1963) Proton tunneling in DNA and its biological implications. Rev Mod Phys 35:724–732
23. Löwdin P-O (1966) "Quantum genetics and the aperiodic solid: Some aspects on the biological problems of heredity, mutations, aging, and tumors in view of the quantum theory of the DNA molecule. " in Advances in Quantum Chemistry: Ed P.-O. Löwdin. Academic Press, New York, NY; London, pp 213–360
24. Polo DS, Mendieta-Moreno J, Trabada DG, Mendieta J, Ortega J (2019) Proton transfer in guanine-cytosine base pairs in B-DNA. J. Chem. Theor. Comput., 15б 6984-6991
25. Brovarets OO, Hovorun DM (2020) Tautomeric hypothesis: To be or not to be? Quantum-mechanical verdict. Ukr Biochem J 92:124–126
26. Slocombe L, Al-Khalili JS, Sacchi M (2021) Quantum and classical effects in DNA point mutations: Watson–Crick tautomerism in AT and GC base pairs. Phys Chem Chem Phys 23:4141–4150
27. Ceron-Carrasco JP, Requena A, Zuniga J, Michaux C, Perpete EA, Jacquemin D (2009) Intermolecular proton transfer in microhydrated guanine-cytosine base pairs: A new mechanism for spontaneous mutation in DNA. J Phys Chem A 113:10549–10556
28. Brovarets' OO, Hovorun DM (2015) New structural hypostases of the A·T and G·C Watson-Crick DNA base pairs caused by their mutagenic tautomerisation in a wobble manner: A QM/QTAIM prediction. RSC Adv 5:99594–99605
29. Brovarets' OO, Oliynyk TA, Hovorun DM (2019) Novel tautomerisation mechanisms of the biologically important conformers of the reverse Löwdin, Hoogsteen, and reverse Hoogsteen G*·C* DNA base pairs *via* proton transfer: A quantum-mechanical survey. Front Chem 7:597
30. Brovarets' OO, Muradova A, Hovorun DM (2020) A quantum-mechanical looking behind the scene of the classical G·C nucleobase pairs tautomerization. Front Chem 8:574454
31. Brovarets' OO, Muradova A, Hovorun DM (2021) Novel mechanisms of the conformational transformations of the biologically important G·C nucleobase pairs in Watson-Crick, Hoogsteen and wobble configurations *via* the mutual rotations of the bases around the intermolecular H-bonds: A QM/QTAIM study. RSC. Adv 11:25700–25730
32. Frisch, M.J., Trucks, G.W., Schlegel, H.B., Scuseria, G.E., Robb, M.A., & Cheeseman,J.R., … Pople, J.A. (2010). GAUSSIAN 09 (Revision B.01). Wallingford CT: Gaussian Inc

33. Parr RG, Yang W (1989) Density-functional theory of atoms and molecules. Oxford University Press, Oxford
34. Lee C, Yang W, Parr RG (1988) Development of the Colle-Salvetti correlation-energy formula into a functional of the electron density. Phys Rev B 37:785–789
35. Hariharan PC, Pople JA (1973) The influence of polarization functions on molecular orbital hydrogenation energies. Theor Chim Acta 28:213–222
36. Krishnan R, Binkley JS, Seeger R, Pople JA (1980) Self-consistent molecular orbital methods. XX. A basis set for correlated wave functions. J Chem Phys 72:650–654
37. Matta CF (2010) How dependent are molecular and atomic properties on the electronic structure method? Comparison of Hartree-Fock, DFT, and MP2 on a biologically relevant set of molecules. J Comput Chem 31:1297–1311
38. Brovarets' OO, Zhurakivsky RO, Hovorun DM (2015) DPT tautomerisation of the wobble guanine·thymine DNA base mispair is not mutagenic: QM and QTAIM arguments. J Biomol Struct & Dynam 33:674–689
39. Brovarets' OO, Hovorun DM (2010) How stable are mutagenic tautomers of the DNA bases? Biopol. Cell 26:72–76
40. Peng C, Ayala PY, Schlegel HB, Frisch MJ (1996) Using redundant internal coordinates to optimize equilibrium geometries and transition states. J Comput Chem 17:49–56
41. García-Moreno BE, Dwyer JJ, Gittis AG, Lattman EE, Spencer DS, Stites WE (1997) Experimental measurement of the effective dielectric in the hydrophobic core of a protein. Biophys Chem 64:211–224
42. Bayley ST (1951) The dielectric properties of various solid crystalline proteins, amino acids and peptides. Trans Faraday Soc 47:509–517
43. Frisch MJ, Head-Gordon M, Pople JA (1990) Semi-direct algorithms for the MP2 energy and gradient. Chem Phys Lett 166:281–289
44. Kendall RA, Dunning TH Jr, Harrison RJ (1992) Electron affinities of the first-row atoms revisited. Systematic basis sets and wave functions. J Chem Phys 96:6796–6806
45. Bader RF (1990) W. Atoms in molecules: A quantum theory. Oxford University Press, Oxford
46. Keith TA (2010) AIMAll (Version 10.07.01). Retrieved from aim.tkgristmill.com
47. Matta CF, Hernández-Trujillo J (2003) Bonding in polycyclic aromatic hydrocarbons in terms of the electron density and of electron delocalization. J Phys Chem A 107:7496–7504
48. Matta CF, Castillo N, Boyd RJ (2006) Atomic contributions to bond dissociation energies in aliphatic hydrocarbons. J Chem Phys 125:20, 204103
49. Cukrowski I, Matta CF (2010) Hydrogen–hydrogen bonding: A stabilizing interaction in strained chelating rings of metal complexes in aqueous phase. Chem Phys Lett 499:66–69
50. Lecomte C, Espinosa E, Matta CF (2015) On atom–atom 'short contact' bonding interactions in crystals. IUCrJ 2:161–163

Tables

Table 1. Energetic and polar characteristics of the conformational and tautomeric transformations of the G·C base pairs *via* the mutual rotations of the G and C bases around the intermolecular H-bonds and proton transfer along the intermolecular H-bonds, respectively, obtained at the MP2/6-311++G(2df,pd)//B3LYP/6-311++G(d,p) level of theory in vacuum under normal conditions (T=298.15 K) (see Fig. 1).

Conformational or tautomeric transformations	ΔG^a	ΔE^b	$\Delta\Delta G_{TS}^c$	$\Delta\Delta E_{TS}^d$	μ_{TS}^e
1. $G^{*}\cdot C^{*}(WC)\leftrightarrow G^{*}\cdot C^{*}(rw_{WC/H})\leftrightarrow G^{*t}\cdot C(rw_{WC/H})\leftrightarrow G^{*t}\cdot C(rw_{H})_{\uparrow}\leftrightarrow G^{*}_{N7}\cdot C^{*}(rw_{H})_{\uparrow}\leftrightarrow G^{*}_{N7}\cdot C^{*}(w_{H})_{\uparrow}\leftrightarrow G^{*t}\cdot C^{*}_{O2}(w_{H})_{\uparrow}\leftrightarrow G^{*t}\cdot C^{*}_{O2}(rw_{H})_{\uparrow}$					
$G^{*}\cdot C^{*}(WC)\leftrightarrow G^{*}\cdot C^{*}(rw_{WC/H})$	7.63	10.21	10.05	11.08	6.44
$G^{*}\cdot C^{*}(rw_{WC/H})\leftrightarrow G^{*t}\cdot C(rw_{WC/H})$	-2.06	-2.21	7.98	6.31	10.48
$G^{*t}\cdot C(rw_{WC/H})\leftrightarrow G^{*t}\cdot C(rw_{H})_{\uparrow}$	-1.87	-3.21	1.81	0.61	8.84
$G^{*t}\cdot C(rw_{H})_{\uparrow}\leftrightarrow G^{*}_{N7}\cdot C^{*}(rw_{H})_{\uparrow}$	11.39	11.86	9.87	12.74	11.12
$G^{*}_{N7}\cdot C^{*}(rw_{H})_{\uparrow}\leftrightarrow G^{*}_{N7}\cdot C^{*}(w_{H})_{\uparrow}$	3.25	3.12	13.31	13.06	9.46
$G^{*}_{N7}\cdot C^{*}(w_{H})_{\uparrow}\leftrightarrow G^{*t}\cdot C^{*}_{O2}(w_{H})_{\uparrow}$	-0.31	-0.64	1.67	4.11	7.54
$G^{*t}\cdot C^{*}_{O2}(w_{H})_{\uparrow}\leftrightarrow G^{*t}\cdot C^{*}_{O2}(rw_{H})_{\uparrow}$	3.93	4.69	8.53	9.22	4.25
2. $G^{*}\cdot C^{*}(rWC)\leftrightarrow G^{*}\cdot C^{*}(w_{WC/H})\leftrightarrow G^{*t}\cdot C^{*}_{O2}(w_{WC/H})\leftrightarrow G^{*t}\cdot C^{*}_{O2}(rw_{WC})_{\downarrow}/\leftrightarrow G^{*t}\cdot C^{*}_{O2}(w_{H})_{\uparrow}$					
$G^{*}\cdot C^{*}(rWC)\leftrightarrow G^{*}\cdot C^{*}(w_{WC/H})$	8.40	11.16	10.29	11.67	6.09
$G^{*}\cdot C^{*}(w_{WC/H})\leftrightarrow G^{*t}\cdot C^{*}_{O2}(w_{WC/H})$	16.10	15.64	18.98	20.76	6.73
$G^{*t}\cdot C^{*}_{O2}(w_{WC/H})\leftrightarrow G^{*t}\cdot C^{*}_{O2}(rw_{WC})_{\downarrow}$	-7.66	-8.47	2.85	1.79	2.50
$G^{*t}\cdot C^{*}_{O2}(w_{WC/H})\leftrightarrow G^{*t}\cdot C^{*}_{O2}(w_{H})_{\uparrow}$	-8.47	-9.73	1.20	0.23	7.55
3. $G^{*}\cdot C^{*t}(rWC)\leftrightarrow G^{*}\cdot C^{*t}(w_{WC/H})\leftrightarrow G^{*t}\cdot C^{*t}_{O2}(w_{WC/H})\leftrightarrow G^{*t}\cdot C^{*t}_{O2}(w_{H})_{\downarrow}\leftrightarrow G^{*t}\cdot C^{*t}_{O2}(rw_{H})_{\downarrow}/\leftrightarrow G^{*t}\cdot C^{*t}_{O2}(rw_{WC})_{\downarrow}\leftrightarrow G^{*t}\cdot C^{*t}_{O2}(w_{WC})_{\downarrow}$					
$G^{*}\cdot C^{*t}(rWC)\leftrightarrow G^{*}\cdot C^{*t}(w_{WC/H})$	3.48	6.52	6.66	8.03	3.65
$G^{*}\cdot C^{*t}(w_{WC/H})\leftrightarrow G^{*t}\cdot C^{*t}_{O2}(w_{WC/H})$	11.23	9.53	13.06	13.12	3.88
$G^{*t}\cdot C^{*t}_{O2}(w_{WC/H})\leftrightarrow G^{*t}\cdot C^{*t}_{O2}(w_{H})_{\downarrow}$	7.90	11.14	7.69	8.87	4.21
$G^{*t}\cdot C^{*t}_{O2}(w_{H})_{\downarrow}\leftrightarrow G^{*t}\cdot C^{*t}_{O2}(rw_{H})_{\downarrow}$	-8.14	-9.88	1.63	0.21	8.04

$G^{*t}{\cdot}C^{*t}{}_{O2}(rw_H)_{\downarrow}$					
$G^{*t}{\cdot}C^{*t}{}_{O2}(w_{WC/H}) \leftrightarrow G^{*t}{\cdot}C^{*t}{}_{O2}(rw_{WC})_{\downarrow}$	-2.50	-2.33	4.47	6.56	2.94
$G^{*t}{\cdot}C^{*t}{}_{O2}(rw_{WC})_{\downarrow} \leftrightarrow G^{*t}{\cdot}C^{*t}{}_{O2}(w_{WC})_{\downarrow}$	7.80	10.70	7.82	7.96	4.60

[a]Relative Gibbs free energy of the formed G·C base pair (T=298.15 K), kcal•mol^{-1}; [b]Relative electronic energy of the formed G·C base pair, kcal•mol^{-1}; [c]Relative Gibbs free energy of the TS of the conformational or tautomeric transformation (T=298.15 K), kcal•mol^{-1}; [d]Relative electronic energy of the TS of the conformational or tautomeric transformation, kcal•mol^{-1}; [e]Dipole moment of the TS, D. Symbols "$_{\uparrow}$" and "$_{\downarrow}$" designate shifting up or down, respectively, of the base on the right relatively the base on the left within the G·C base pair.

Table 1. (continued)

Conformational or tautomeric transformations	ΔG^a	ΔE^b	$\Delta\Delta G_{TS}{}^c$	$\Delta\Delta E_{TS}{}^d$	$\mu_{TS}{}^e$
d) $G^{*t}{\cdot}C^{*}(rH) \leftrightarrow G^{*t}{\cdot}C^{*}(w_{WC/H}) \leftrightarrow G^{*}{\cdot}C^{*}{}_{O2}(w_{WC/H}) \leftrightarrow G^{*}{\cdot}C^{*}{}_{O2}(w_{WC})_{\uparrow} / \leftrightarrow G^{*}{\cdot}C^{*}{}_{O2}(w_H)_{\downarrow}$					
$G^{*t}{\cdot}C^{*}(rH) \leftrightarrow G^{*t}{\cdot}C^{*}(w_{WC/H})$	7.05	9.12	8.77	9.28	7.13
$G^{*t}{\cdot}C^{*}(w_{WC/H}) \leftrightarrow G^{*}{\cdot}C^{*}{}_{O2}(w_{WC/H})$	13.70	13.29	17.21	18.89	7.27
$G^{*}{\cdot}C^{*}{}_{O2}(w_{WC/H}) \leftrightarrow G^{*}{\cdot}C^{*}{}_{O2}(w_{WC})_{\uparrow}$	-8.74	-9.01	2.78	2.00	6.00
$G^{*}{\cdot}C^{*}{}_{O2}(w_{WC/H}) \leftrightarrow G^{*}{\cdot}C^{*}{}_{O2}(w_H)_{\downarrow}$	-4.56	-5.32	4.43	3.52	3.22
e) $G^{*t}{\cdot}C^{*t}(rH) \leftrightarrow G^{*t}{\cdot}C^{*t}(w_{WC/H}) \leftrightarrow G^{*}{\cdot}C^{*t}{}_{O2}(w_{WC/H}) \leftrightarrow G^{*}{\cdot}C^{*t}{}_{O2}(w_{WC})_{\uparrow} / \leftrightarrow G^{*}{\cdot}C^{*t}{}_{O2}(rw_H)_{\downarrow} \leftrightarrow G^{*}{\cdot}C^{*t}{}_{O2}(w_H)_{\downarrow}$					
$G^{*t}{\cdot}C^{*t}(rH) \leftrightarrow G^{*t}{\cdot}C^{*t}(w_{WC/H})$	4.86	6.44	6.65	6.68	5.02
$G^{*t}{\cdot}C^{*t}(w_{WC/H}) \leftrightarrow G^{*}{\cdot}C^{*t}{}_{O2}(w_{WC/H})$	10.61	10.10	13.78	15.01	5.93
$G^{*}{\cdot}C^{*t}{}_{O2}(w_{WC/H}) \leftrightarrow G^{*}{\cdot}C^{*t}{}_{O2}(w_{WC})_{\uparrow}$	-8.10	-8.45	3.30	3.07	6.36
$G^{*}{\cdot}C^{*t}{}_{O2}(w_{WC/H}) \leftrightarrow G^{*}{\cdot}C^{*t}{}_{O2}(rw_H)_{\downarrow}$	-2.61	-2.46	3.42	4.49	2.67
$G^{*}{\cdot}C^{*t}{}_{O2}(rw_H)_{\downarrow} \leftrightarrow G^{*}{\cdot}C^{*t}{}_{O2}(w_H)_{\downarrow}$	9.40	11.86	11.32	11.90	5.59

Designations: see above.

Figures

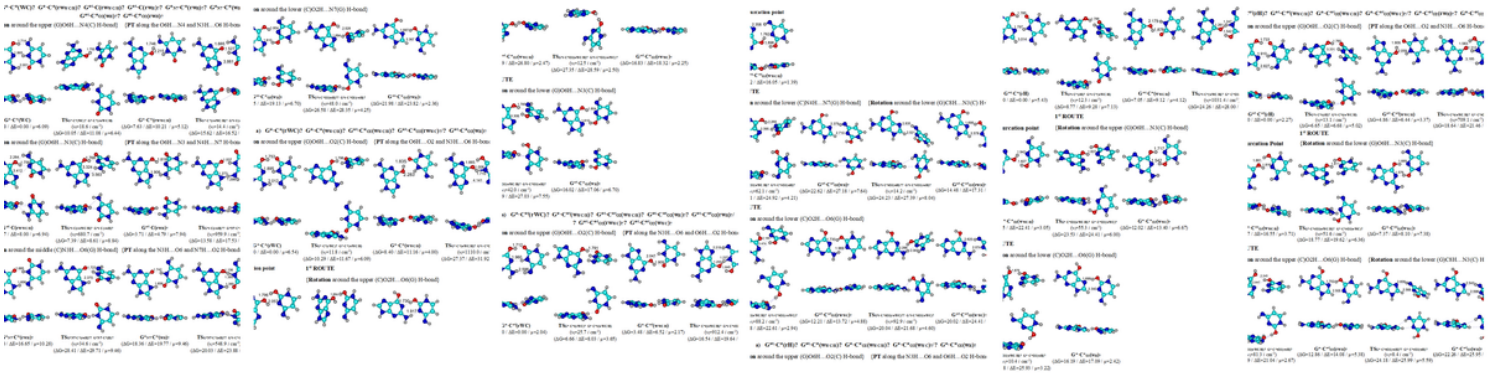

Figure 1

Conformationally-tautomeric transformations of the Lowdin G*·C*(WC), reverse Lowdin G*·C*(rWC), G*·C*^{t}(rWC) and reverse Hoogsteen G*^{t}·C*(rH), G*^{t}·C*^{t}(rH) base pairs *via* the mutual rotations of the bases around the intermolecular H-bond and proton transfer (PT) along the intermolecular H-bonds, obtained at the MP2/6-311++G(2df,pd)//B3LYP/6-311++G(d,p) level of theory in vacuum under normal conditions (ΔG – relative Gibbs free energy (T=298.15 K), kcal·mol^{-1}; ΔE – electronic energy, kcal·mol^{-1}; v_i – imaginary frequency at the TS; μ – dipole moment of the complex, D).

Intermolecular AH…B H-bonds are designated by the dotted lines, their lengths H…B are presented in Angstroms. Symbols "$_{\uparrow}$"and "$_{\downarrow}$" mean displacement of the base on the right up and down relatively the base on the left, accordingly.